

Variety of stylolites' morphologies and statistical characterization of the amount of heterogeneities in the rock

Alexandre Brouste^a, François Renard^{b,c,*}, Jean-Pierre Gratier^b, Jean Schmittbuhl^d

^a Laboratoire de Modélisation et de Calcul, Université Joseph Fourier, BP 53, 38041 Grenoble, France

^b Laboratoire de Géophysique Interne et Tectonophysique, CNRS, Université Joseph Fourier, BP 53, 38041 Grenoble, France

^c Physics of Geological Processes, University of Oslo, Norway

^d UMR 7516, Institut de Physique du Globe de Strasbourg, 5 rue René Descartes, F-67084 Strasbourg Cedex, France

Received 7 June 2006; received in revised form 31 August 2006; accepted 20 September 2006

Available online 28 November 2006

Abstract

The surface roughness of several stylolites in limestones was measured using high-resolution laser profilometry. The 1D signals obtained were statistically analyzed to determine the scaling behavior and calculate a roughness exponent, also called Hurst exponent. Statistical methods based on the characterization of a single Hurst exponent imply strong assumptions on the mathematical characteristics of the signal: the derivative of the signal (or local increments) should be stationary and has finite variance. The analysis of the measured stylolites shows that these properties are not always verified simultaneously. The stylolite profiles show persistence and jumps and several stylolites are not regular, with alternating regular and irregular portions. A new statistical method is proposed here, based on a non-stationary but Gaussian model, to estimate the roughness of the profiles and quantify the heterogeneity of stylolites. This statistical method is based on two parameters: the local roughness (H), which describes the local amplitude of the stylolite, and the amount of irregularities on the signal (μ), which can be linked to the heterogeneities initially present in the rock before the stylolite formed. Using this technique, a classification of the stylolites in two families is proposed: those for which the morphology is homogeneous everywhere and those with alternating regular and irregular portions.

© 2006 Elsevier Ltd. All rights reserved.

Keywords: Stylolites; Roughness; Scaling analysis; Heterogeneity

1. Introduction

The geometrical characterization of rough profiles or surfaces is a widespread problem in various geological examples such as erosion patterns (Dunne, 1980; Cerasi et al., 1995), multiphase fluid percolation in porous rocks (Rubio et al., 1989), fractures (Schmittbuhl et al., 1993), or stylolites (Renard et al., 2004). In these studies, the scaling behavior of various data sets was investigated, showing that the statistics at one scale could be extrapolated to another scale using a power-law relationship.

For a self-affine function $h(x)$, a scaling relationship is defined when the signal follows a power-law relationship under a dilation of a factor λ

$$h(\lambda x) = \lambda^D h(x) \quad (1)$$

where x is the spatial coordinate and h is a scalar field, λ is the scaling scalar, and D is the scaling exponent.

Applying this property to 1D discrete signals involves working on the increments $\delta h(x)$ of the function h . The self-similar property of a 1D data set $h(x)$ emerges when the increments of the signal follow

$$\delta(h(\lambda x)) = \lambda^H \delta(h(x)) \quad (2)$$

where H is the so-called Hurst exponent (Feder, 1988; Meakin, 1998).

* Corresponding author. Laboratoire de Géophysique Interne et Tectonophysique, CNRS, Université Joseph Fourier, BP 53, 38041 Grenoble, France. Tel.: +33 476 82 80 88; fax: +33 476 82 81 01.

E-mail address: francois.renard@ujf-grenoble.fr (F. Renard).

This scaling approach is based on two assumptions on the mathematical properties of the signal. First, increments of the signal have finite variance distribution and, second they are stationary, which means that the statistics are independent of the position along the signal. In the case of a signal with increments that follow a Gaussian distribution (that has a finite variance by definition), the roughness of the signal can be deduced from the scaling exponent.

For a function $h(x)$ with the property:

$$|h(x) - h(y)| \leq C|x - y|^{H_0}, \quad (3)$$

where x and y are two different points along the signal and C is a constant, H_0 is defined as the Hölder exponent (Daubechies, 1992). When the increments of a signal are Gaussian and stationary, the Hölder exponent is equal to the Hurst exponent.

In this contribution, the assumption of Gaussian stationary increments of several 1D data sets is tested, based on roughness measurements of various stylolites in limestones. We show that these profiles do not verify the Gaussian stationary increments property, and we propose a new technique to characterize the statistics of these signals by introducing two parameters: the *localized* roughness exponent H , and a second parameter μ , which characterizes the quantity of irregularities in the system at all scales. Applied to stylolites, this parameter can be used to quantify the degree of heterogeneity in the rock initially present before the stylolitization process. We also show that heterogeneities have an effect only above a millimeter scale.

We first present some examples showing how heterogeneities determine the location of some stylolite peaks. Then the two-parameter statistical description of stylolite roughness is used to help characterize such heterogeneities.

2. The roughness of stylolites

2.1. Self-similar scaling of stylolites

Stylolites are rough surfaces that develop by stress-enhanced dissolution in crustal rocks (Dunnington, 1954; Park and Schot, 1968; Bathurst, 1971; Bayly, 1986). Anticrack models have been proposed to describe their initial stage of nucleation and propagation as a flat interface (Fletcher and Pollard, 1981; Koehn et al., 2003; Katsman et al., 2006). With time, the stylolites roughen and acquire their typical wavy geometry (Figs. 1 and 2). The wide range of morphological geometries of such surfaces makes them difficult to characterize using a simple scaling approach. However, it has been shown that stylolites have self-similar scaling properties (Karcz and Scholz, 2003; Renard et al., 2004; Schmittbuhl et al., 2004). These studies are based on the assumption that the morphological statistics of the stylolites do not vary laterally along the plane of the interface.

Here, the topography of stylolites in limestones was measured using high-resolution laser profilometers that acquire (1 + 1)D roughness profiles (Fig. 2). Some stylolites were split open to reveal the complex 2D geometry of their surface.

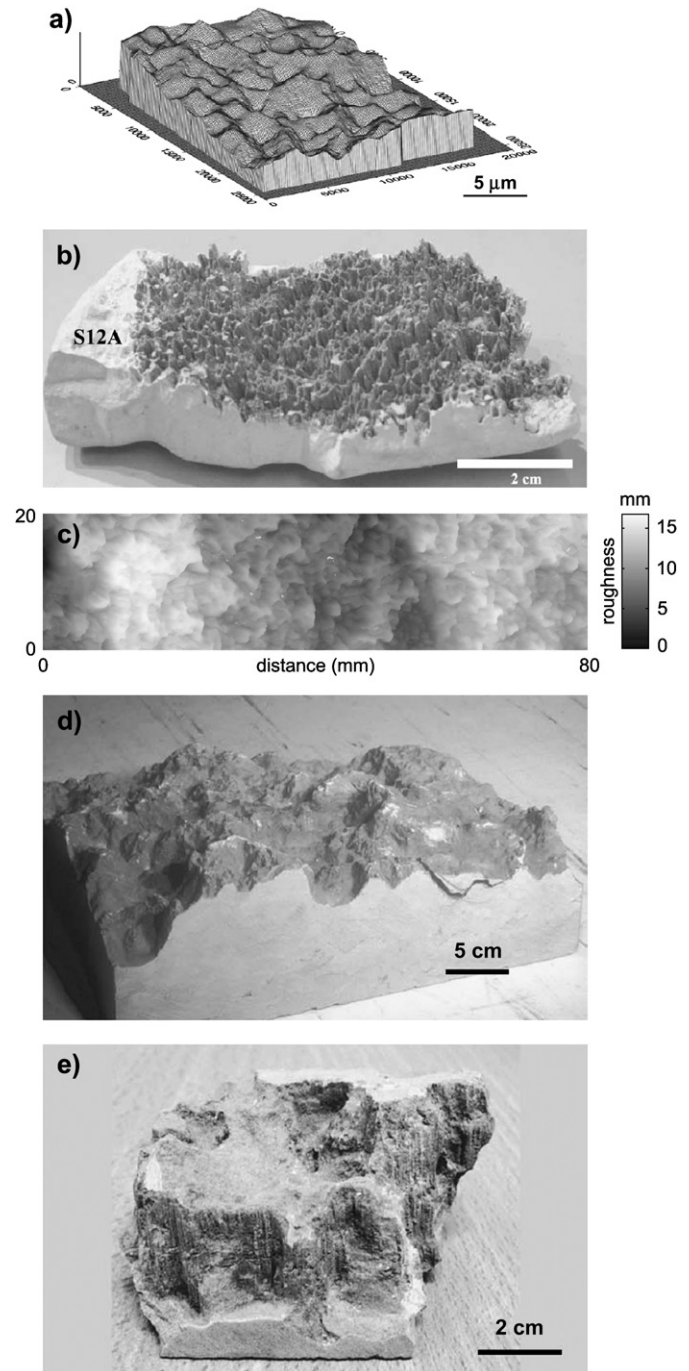


Fig. 1. Various shapes of stylolites. a) Digital elevation model of a microstylolite measured at the contact between experimentally deformed quartz grains (after Gratier et al., 2005, isotropic scale). b) 2D stylolite surface S12A in a limestone. c) Roughness field of the surface S12A measured using a laser profilometer (Renard et al., 2004). d) Stylolite S3b showing local variations in roughness, with alternating smooth and rougher areas. Such lateral roughness variations are a good visual indicator that the roughness statistics are not the same all along the profiles. e) Stylolite in limestone with vertical peaks showing strong lateral variations in height. It was not possible to measure the roughness of such stylolites because of local overhangs.

Using this method, described in Renard et al. (2004), (2 + 1)D maps of stylolite roughness can be obtained with an accuracy of up to 0.003 mm, on a regular grid of 0.03 to 0.125 mm depending on the kind of profilometer used. The

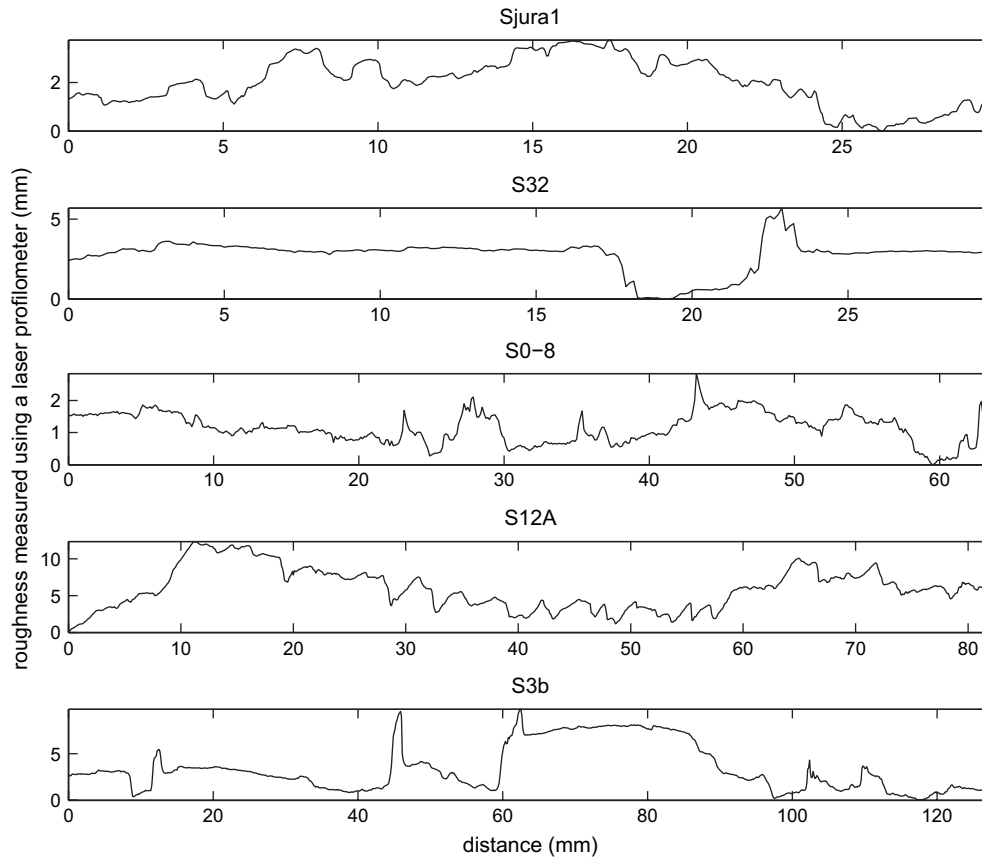


Fig. 2. Examples of the 1D roughness of different stylolites in limestones measured using laser profilometer (see Renard et al. (2004) for the measurement technique). The waviness of the stylolite, characterized by the Hurst exponent H varies from sample to sample. Moreover, within the same stylolite, regions with smooth or wavy roughness can be defined, and characterized by the amount of irregularities defined by the parameter μ (see text). Scales are given in millimeters. The characteristics of each profile are given in Table 1.

(2 + 1)D maps were built by combining (1 + 1)D profiles on a square grid with a constant discretization interval. For each stylolite surface, the result is a (2 + 1)D height field from which the mean plane was removed by a least-square method.

Using these data, stylolitic 1D profiles were found to show two different self-affine regimes at large and small length scales (Fig. 3). Two signal processing techniques were used as follows: the Fourier Power Spectrum (FPS) and the Averaged Wavelet Coefficient (AWC).

FPS decomposition techniques are standard tools used to characterize the scaling behavior of stationary increments signals (Kahane and Lemarié-Rieusset, 1998). Assuming finite variance stationary increments of a signal, the Hurst exponent H (Eq. (2)) can be deduced from the power-law behavior of the Fourier Power Spectrum with

$$\text{FPS}(k) \propto k^{-1-2H} \quad (4)$$

where k is the wave number, the inverse of the wavelength (Barabási and Stanley, 1995).

Wavelet series (or wavelet decompositions) constitutes a powerful tool for processing signals in which different scales are combined (Meyer and Roques, 1993). Various signals can be reconstructed knowing the coefficients of their wavelet

decomposition, and for compactly supported wavelets (Daubechies, 1992) any 1D profile, $h(x)$, can be decomposed into a wavelet series having the following summation:

$$h(x) = \sum_{j=0}^{+\infty} \sum_{i=0}^{2^j-1} c_{j,i} \psi(2^j x - i) \quad (5)$$

where $c_{j,i}$ are the wavelet coefficients indexed by (j,i) and ψ is the so-called mother wavelet (generating all the wavelets by expansion of a factor 2^j and by a translation i).

Using this method, the self-similar behavior of a signal emerges as the average wavelet coefficient AWC satisfies

$$\text{AWC}(l) \propto l^{H+0.5}, \quad (6)$$

where l is the spatial wavelength (Simonsen et al., 1998).

These two techniques provide a scaling relationship and the Hurst exponent is directly related to the slope of the spectra. In the case of a signal with Gaussian and stationary increments, the Hölder exponent is equal to the Hurst exponent.

In stylolites, these two signal processing techniques give the same Hurst exponent (Eq. (2)), $H = 0.5$ for the large length scales and $H = 1.1$ for small length scales (Fig. 3, see also Renard et al., 2004).

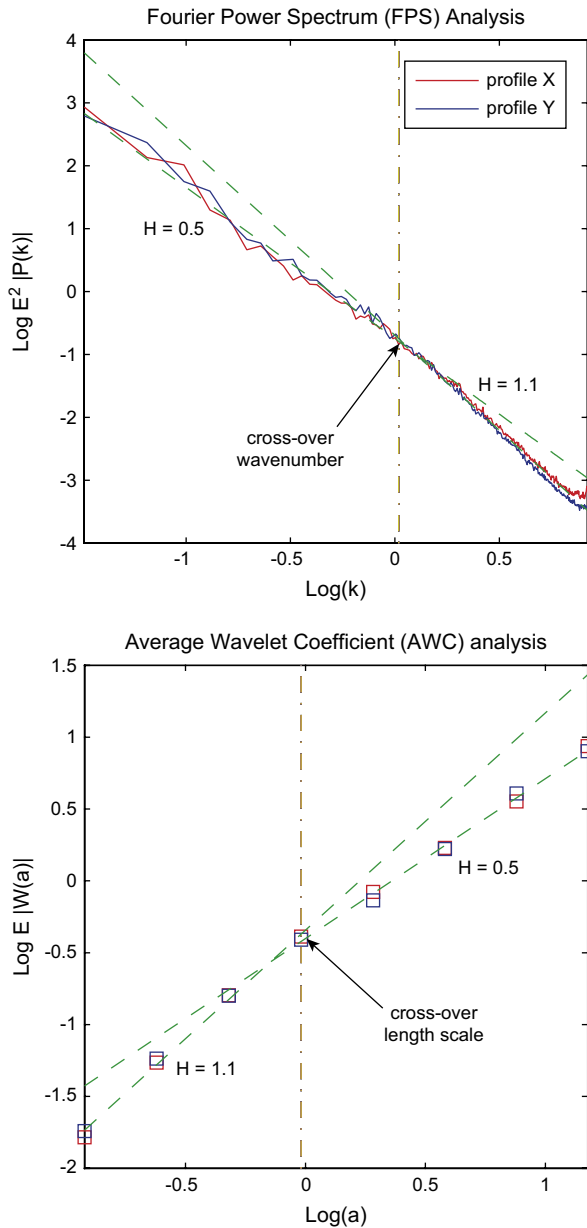


Fig. 3. FPS (top) and AWC (bottom) for the stylolite Sjura1. These two independent scaling methods show that there is a crossover at ~ 1 mm between the small wavelengths ($H \sim 1.1$) and the large wavelengths ($H \sim 1.5$).

The measurements also show that a sharp crossover length scale close to the millimeter scale separates the two regimes. This characteristic length scale has been interpreted as a crossover length emerging from the competition between two forces: surface tension dominates at small wavelengths, whereas elastic interactions dominate at large wavelengths (Renard et al., 2004; Schmittbuhl et al., 2004).

Using the same data sets, it can also be shown that a stylolite can be wavy at one point and rather flat at another point (Fig. 2), suggesting that the statistical properties vary along the profiles. Therefore, the Gaussian stationary increments hypothesis must be called into question. This spatial variation in statistical properties along a single stylolite is not accounted for in current models of stylolite roughening.

2.2. Heterogeneities along stylolites

Various examples both from nature and experiments show that heterogeneities in rocks help either to localize dissolution pits or to deflect the dissolution surface along a single stylolite at all scales. Fig. 4a shows experimental microstylolites along quartz grains (Gratier et al., 2005). Dissolution pits (Fig. 4b) are systematically located at the bottom of each conical-shaped stylolite structure. Due to the fit of the two opposite grain surfaces, the pits of the lower grain stylolite surface are located just in front of the stylolitic peak of the upper grain and vice versa. The explanation is that pits develop at intersections of crystal dislocations with the grain surface and determine the stylolite peak location.

Fig. 4c shows the indenting of a mineral (quartz) by another mineral (mica). In this case, the mica grains along the dissolution surface are responsible for the local dissolution peaks. Mica distribution determines the location of the peaks.

The same geometry may be observed along columnar stylolites in limestones (Fig. 4d). However, the interpretation is different as the two parts of the rock have the same composition. In this case, the geometry of the columnar stylolite is probably determined by preexisting microfractures as is clearly the case in the example shown in Fig. 4e where a fracture controls the shape of the peak. Finally, Fig. 4f shows several dissolution seams that are deflected by hard objects: pyrite (black) or quartz pressure shadows (white). In this case, the hard objects located in the dissolution plane deflect it, thereby contributing to roughening of the dissolution surface.

All these examples show that the location of some stylolite peaks is not purely random but rather partially controlled by the distribution of heterogeneities. The statistical properties of stylolites should depend on the distribution of these heterogeneities, and therefore vary in space along a single stylolite. It would appear relevant to integrate the presence of non-uniformly distributed heterogeneities at all scales in the modeling of stylolites and test their potential effect on the final geometry.

3. A two-parameter statistical description of the roughness of 1D stylolite profiles

The wide range of morphologies of stylolites (Fig. 1) and the alternating smooth and irregular portions of the same stylolite (Figs. 2 and 5a) suggest that the Gaussian stationary increments assumption should be tested. In this section we show that it is not possible to obtain all stylolite morphologies from a single parameter scaling relationship (e.g. a Hurst exponent).

Fig. 5b represents the increments of a 1D stylolite. These increments are calculated as the height difference between two successive points, and therefore represent a first order derivative of the original signal of Fig. 5a. In this incremental signal, the existence of many large jumps and long tails in the histogram (Fig. 5c) differentiates the signal from a synthetic fractional Gaussian noise signal (Fig. 5h). Therefore, the Gaussian self-similar stationary increments property can be excluded for stylolite signals and a simple scaling

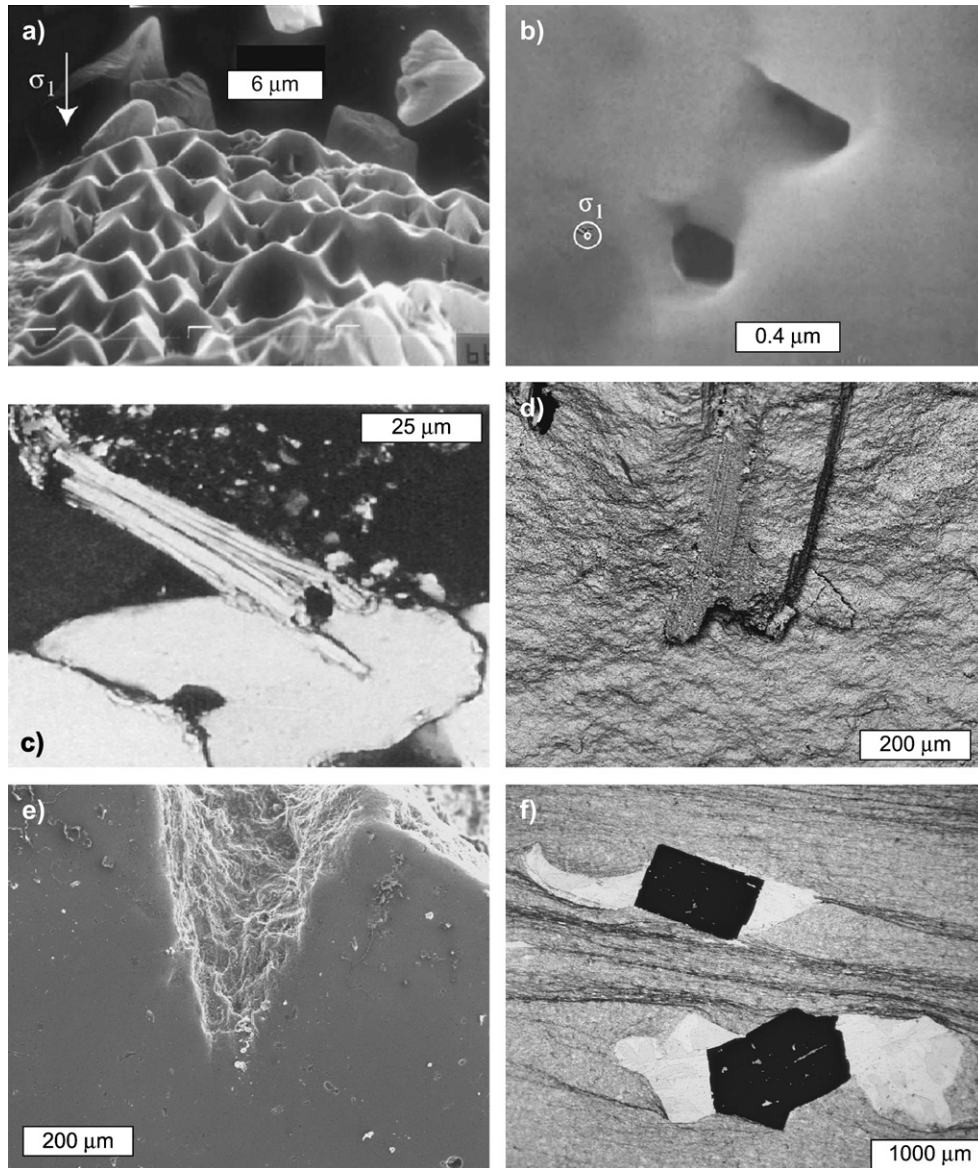


Fig. 4. Heterogeneities associated with stylolites. a,b) Microstylolite on a quartz grain (Gratier et al., 2005) and zoom on two dislocation pits where deformation is localized. c) Mica indenting a quartz grain in a North Sea Sandstone and showing a wavy interface at the grain scale. d,e) Zoom on stylolite peaks in the sample Sjur1. f) Dissolution seams (“flat” stylolites) deflected by pyrite crystals and quartz pressure shadows in a metamorphic schist from Bourg d’Oisans (Alps, France).

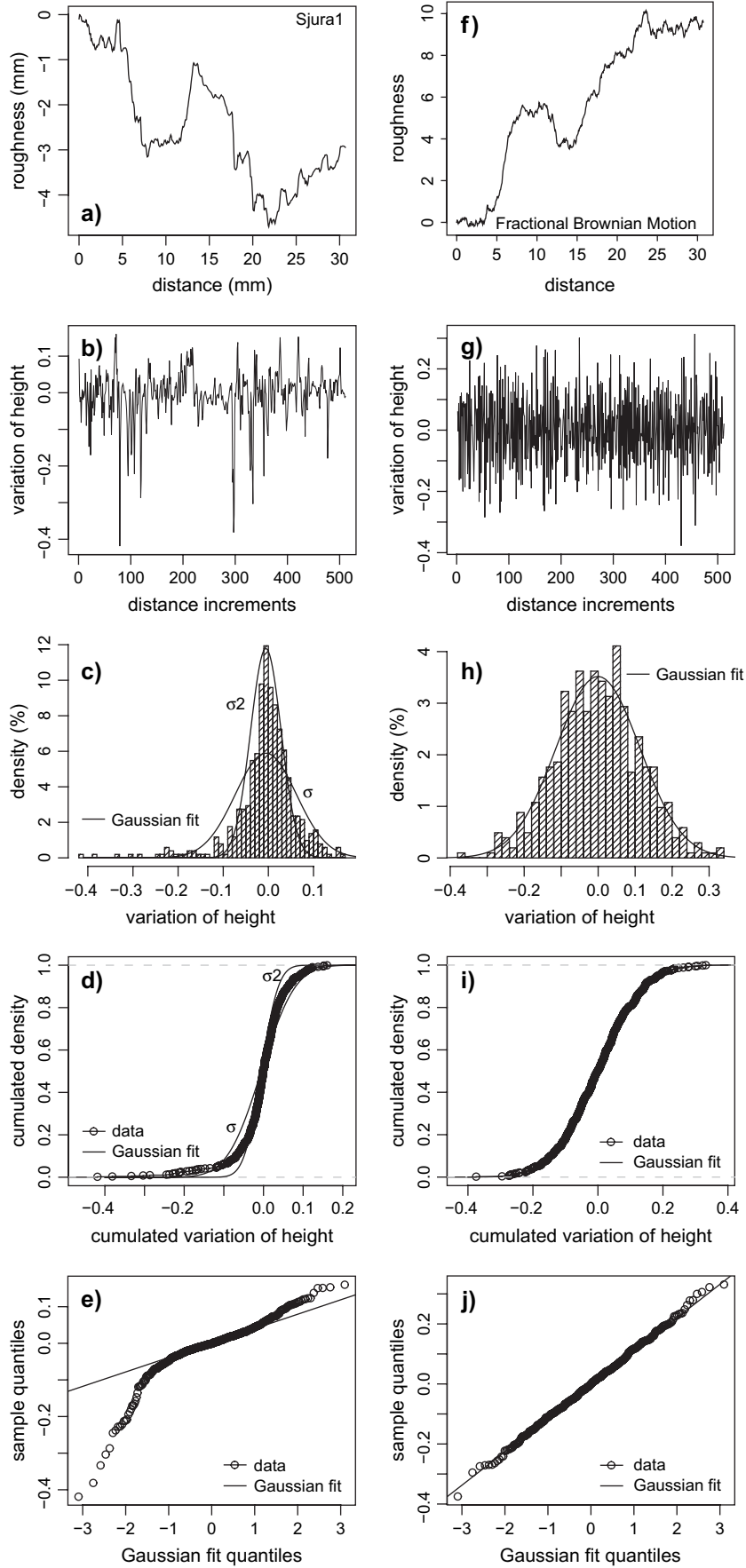
relationship using a single Hurst exponent is not sufficient to explain the measured signals. The following section proposes a new technique that can accommodate the large jumps of Fig. 5b so that it can be applied to stylolites. This analysis has been tested on all the available stylolites’ surfaces and shows similar properties.

3.1. The Simple Branching Process Wavelet Series method

Mathematicians commonly use two different techniques to deal with the large jumps similar to those shown in Fig. 5b. The first technique is to select a non-Gaussian self-similar stationary increment model with infinite variance, also called stable Lévy motion (Samorodnitsky and Taqqu, 1994). Stable

Lévy motions contain two parameters: the frequency of the jumps and the average size of these jumps. Applied to stylolites, microfractures’ densities in the rocks can be associated with the frequency of jumps for instance and estimated by specific methods. However, in such models, the roughness cannot be identified from the scaling relationship because the roughness and the scaling exponents are not similar. The Lévy models are avoided in the following discussion.

The second technique is a non-stationary Gaussian model with scaling properties, where the roughness can be estimated. According to Samorodnitsky and Taqqu (1994), neither of these techniques is superior to the other. In the following section, the non-stationary Gaussian model is used and referred to as the Simple Branching Process Wavelet Series (in short SBPWS).



3.2. Construction of SBPWS profiles in one dimension

Simple Branching Processes (also called Galton–Watson processes, see Harris, 1963) are stochastic trees built by an incremental branching process at all scales. In the case of Simple Branching Process Wavelet Series (SBPWS), each node of the tree has the same probability of having either one or two branches (see Fig. 6a). In the following, $1 < \mu < 2$ corresponds to the average number of sons at each node. For a node of the tree, $(2 - \mu)$ represents the probability of having only one branch.

SBPWS models are particular random lacunary wavelet series (Jaffard, 2000) based on simple branching processes. Lacunary refers to the property that only a small number of coefficients in the series are non-vanishing, more precisely those indexed by an elementary branching process and corresponding to the branches of Fig. 6a. SBPWS is defined by

$$\text{SBPWS}(x) = \sum_{j=0}^{\infty} 2^{-jH} \sum_{i \in \mathcal{A}(\mu)} \varepsilon_{j,i} \psi(2^j x - i) \quad (7)$$

where x is the spatial coordinate, H is the fractional parameter, $\mathcal{A}(\mu)$ is the elementary branching process of parameter μ , $\varepsilon_{j,i}$ are a family of independent Gaussian standard random variables and ψ is a wavelet-like function.

Only wavelets with coefficients indexed by the stochastic sub-tree \mathcal{A} (of non-vanishing coefficients) contribute to the roughening of the initial flat profile (see Fig. 6b). Therefore, the stochastic tree process \mathcal{A} locally deforms the 1D profile, at all the tree branches.

In this model, elementary forms of the deformation are given by the shape of the mother-function ψ . A difficulty with modeling a stylolitic structure is to choose the function ψ , which corresponds to the shape of each dissolution increment. However, it has been shown that the statistics of a simulated signal do not depend on the shape of ψ , as long as this function has the same property as an individual wavelet (Brouste, 2006).

In nature, the stylolite shape varies from columnar to conical (Figs. 1 and 4) and these two kinds of shapes might be related to the shape of microscopic increment of dissolution: either rectangular for columnar stylolites, or triangular for the conical ones. As a consequence, a choice must be made in the mathematical modeling between rectangular or triangular increments or a specific parameter used that may express all the intermediary shapes. Moreover, columnar stylolites are rather specific, being associated either with microfractures (Fig. 4d, e) or with non-consolidated material (Gratier et al., 2005). In order to avoid the use of a third parameter, the shape

of the function ψ , which might hide the effect of the two other parameters, a triangular function was chosen for ψ (Fig. 6b, inset). Note that the choice of the shape of this function ψ does not modify the statistical properties of the synthetic signal.

The natural stylolites that were examined in this study can be modeled with such an elementary triangular shape. By varying the parameters H and μ , one can generate synthetic profiles that have stylolite-like patterns (Fig. 7; Appendix A gives the algorithm to build these synthetic stylolites). These synthetic profiles, unlike those generated by previous models, exhibit two important properties of the natural stylolites:

- i) the variability of the roughness between independent stylolite profiles;
- ii) the variability of the roughness within a single profile, with alternating regular and irregular portions.

3.3. Parameters H and μ

The parameters H and μ have distinct visual effects on the synthetic profiles. The irregularities on the whole profile are quantified by the parameter μ : for instance, at the n th order branches, there are, on average, μ^n non-vanishing coefficients and then μ^n branches of the tree, corresponding to μ^n stages of deformation of the initially flat profile. When μ is close to 2, there are irregularities everywhere along the profile. When μ decreases to 1, there are alternating irregular and regular portions along the profile. Finally, when μ is equal to 1, there are no more irregularities along the signal.

The amplitude of the deformation (only where it is deformed) depends on the scale, on a random Gaussian variable, and on a fractional exponent H that can be considered to be a local roughness parameter. In this sense, H is indicative of the nature of the irregularity and the amplitude of the profile variations. When H tends to 0 the profile is irregular and looks “noisy”. This property is also called antipersistence: locally a valley in the signal has a greater probability of being followed by a hill. When H is close to 1, the profile roughness is smoother and a valley or a hill in the signal tends to extend locally. This property is called persistence (Meakin, 1998).

3.4. Measurements of H and μ on a 1D data set

As stated previously, the SBPWS have scaling properties that no longer involve a unique stationary Hurst exponent. SBPWS provides self-affine behavior either in the 1D average wavelet coefficient technique or in the Fourier Power

Fig. 5. a) Laser roughness measurement of a 1D profile from the stylolite Sjur1. b) Local increments of the stylolite Sjur1, corresponding to the first order discrete derivative of profile a). c) Histogram of the increments of b) with the best Gaussian fits represented by the two curves, which have the same standard deviation (σ) and half the standard deviation ($\sigma/2$) of the stylolite data. d) Cumulative distribution function of b). The two lines represent the best Gaussian fits as in b). The large jumps of the local increments and the long tails in the histogram cannot be accounted for using Gaussian stationary statistics (plain curves). e) Quantile–quantile plot that adjusts the sample distribution in d) against the best Gaussian distribution. This corresponds to the difference between the data and the Gaussian estimate of d). For a Gaussian distribution a straight line should be observed. f.) Same plots for a synthetic fractional Brownian motion. In the quantile–quantile plot, the synthetic signal and the Gaussian best fit adjust perfectly on a straight line, showing that the fractional Brownian motion is a Gaussian stationary increments’ signal.

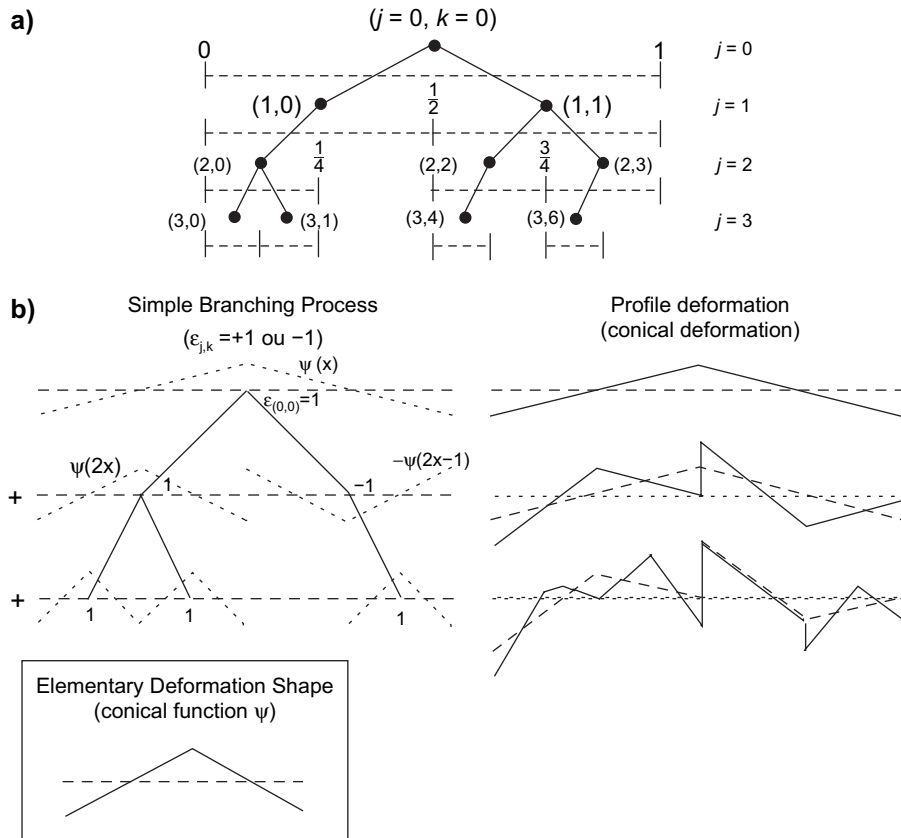


Fig. 6. a) Galton–Watson tree (simple branching process) and indexes for the wavelet construction. b) Construction of a synthetic 1D profile using the Branching Process Wavelet Series. Such technique is used to build the synthetic signals of Fig. 7, using the algorithm given in Appendix A.

Spectrum, and is defined by a power law in both scale and frequency domains, respectively (Brouste, 2006):

$$AWC(l) \propto l^{1-\log_2 \mu/2+H} \tag{8}$$

and

$$FPS(k) \propto k^{-2+\log_2 \mu-2H} \tag{9}$$

where H and μ are the two parameters of the SBPWS method. When $\mu = 2$, Eqs. (8) and (9) are reduced to the Gaussian stationary case described in Eqs. (4) and (6), respectively.

Note that in the SBPWS method, the values of H and μ cannot be determined by a simple regression to the 1D Fourier and AWC spectra, as done previously by Renard et al. (2004), because the following system of equations, whose determinant is equal to zero, is underdetermined

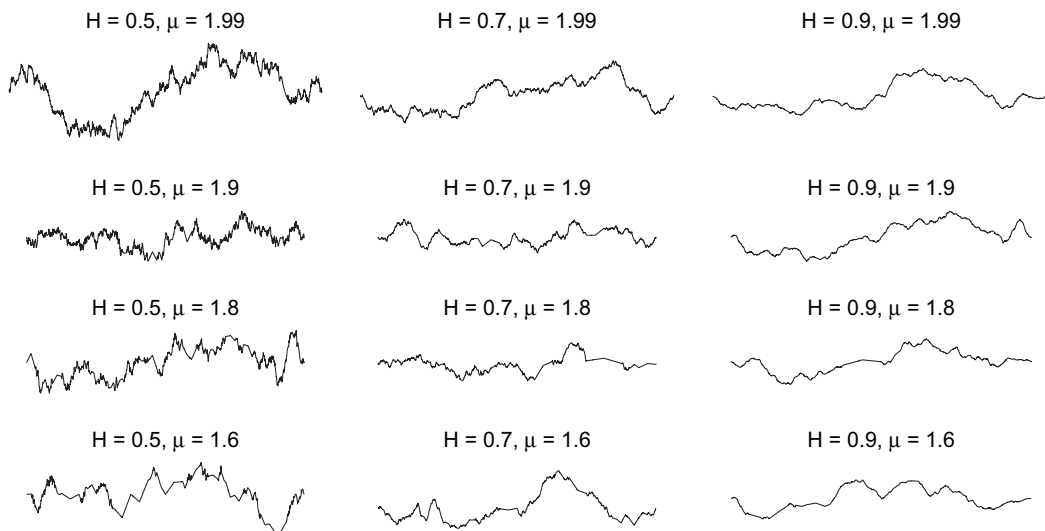


Fig. 7. Simulated stylolites with statistical roughness properties characterized by two parameters. The variability in the stylolite morphology is controlled by H which describes the apparent noisiness (smoothness) of the roughness, and μ which describes the spatial variability (heterogeneities at all scales) along the stylolite.

$$\begin{cases} 2H - 2 + \log_2 \mu = a \\ H - 1 + \log_2 \mu/2 = b \end{cases} \quad (10)$$

Here a and b are the slopes measured by linear regression on the FPS spectrum and on the AWC spectrum, respectively.

Therefore, a more complex tool must be used, such as the s -generalized variations method (Istas and Lang, 1997) to obtain estimated values of H and μ at large and small length scales. This method, detailed in Appendix B, was applied to estimate H and μ in the stylolites that were measured (Table 1).

4. Application to natural stylolites

4.1. Parameters H and μ for the stylolites

To estimate the parameters μ and H , from both sides of the crossover length scale, it is necessary to observe how the estimators of Appendix B behave when the length scale decreases (as n increases), from large scales to small scales through the crossover length scale (Fig. 8a, b). Large length scale values are taken at the crossover length scale and small ones are taken at the discretization scale in order to use the greatest number of points in the two different patterns.

The results presented in Table 1 are based on averaged estimations of a series of 256 to 512 parallel stylolite profiles, each profile being regularly discretized on 512 to 1024 points. This gives the large length scale and the small length scale parameters H and μ for all the stylolites that have been measured.

4.2. Geometrical characterization

Most of the information on μ and H variability belongs to the large length scale parameters (see Table 1). In fact, small length scale parameters have almost similar values (μ from 1.2 to 1.4 and H from 0.6 to 0.85) for all samples except S12A and

Table 1
Large and small length scale scaling exponents of the various stylolites

Stylolite	Origin	H_{small}	μ_{small}	H_{large}	μ_{large}
Sjura1	Jura mountains	0.75	1.3	0.4	1.85
S12A	Vercors mountains	0.2	1	0.3	1.9
S11c	Burgundy mountains	0.7	1.35	1	1.9
S3b	Chartreuse mountains	0.5	1.4	0.3	1.6
S15A	Burgundy	0.6	1.4	0.65	2
S0_8	Jura mountains	0.6	1.3	0.2	1.5
S13A	Burgundy	0.9	1.8	0.55	1.8
S10A	Burgundy	0.85	1.4	1	2
Sdiss1	Experimental microstylolite	0.8	1.25	—	—
Sdiss2	Experimental microstylolite	0.75	1.2	—	—

For more details on the geological characteristics and composition of the stylolites, see Renard et al. (2004) and Gratier et al. (2005) for the experimental microstylolites.

S13A. These results are also found on experimental microstylolites in quartz (Sdiss1 and Sdiss2 in Table 1, Gratier et al., 2005), suggesting that a physical process smoothes the stylolites at small wavelengths.

Plotting the results of the analysis in μ versus H space, one can distinguish between two classes of stylolites at long wavelengths (Fig. 9). A first class, called homogeneous stylolites, contains two kinds of profiles: (i) the almost-everywhere irregular stylolites (Sjura1 or S12A) and (ii) the smooth stylolites (S11C or S10A). For both kinds, the parameter μ is close to 2 (greater than 1.75), which represents few heterogeneities in the rock. Irregular stylolites have a localized roughness parameter H that varies around 0.5 (0.4–0.5 in the results obtained here), contrary to smooth stylolites where H is close to 1. Stylolites of this class can be simulated by dynamic surface growth models such as the Langevin growth equations (Renard et al., 2004; Schmittbuhl et al., 2004) because profiles have the same kind of irregularity almost everywhere.

The second class of stylolites, called heterogeneous stylolites, contains a variety of morphologies. In this case the parameter μ is close to 1.5 (stylolites S3b or S0_8). These

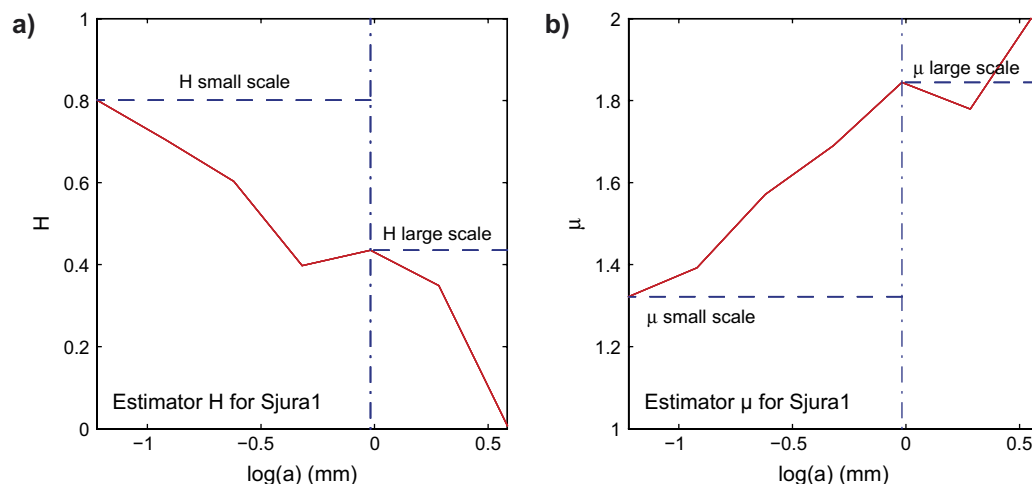


Fig. 8. a, b) Estimators of μ and H for the stylolite Sjura1 at small length scales and large length scale. As the length scale a decreases (n increases in the equations of Appendix B, where n represents the level of branching in Fig. 6), the estimated values converge respectively to H and μ just above the crossover length scale for large length scales and as allowed by the precision for small length scales.

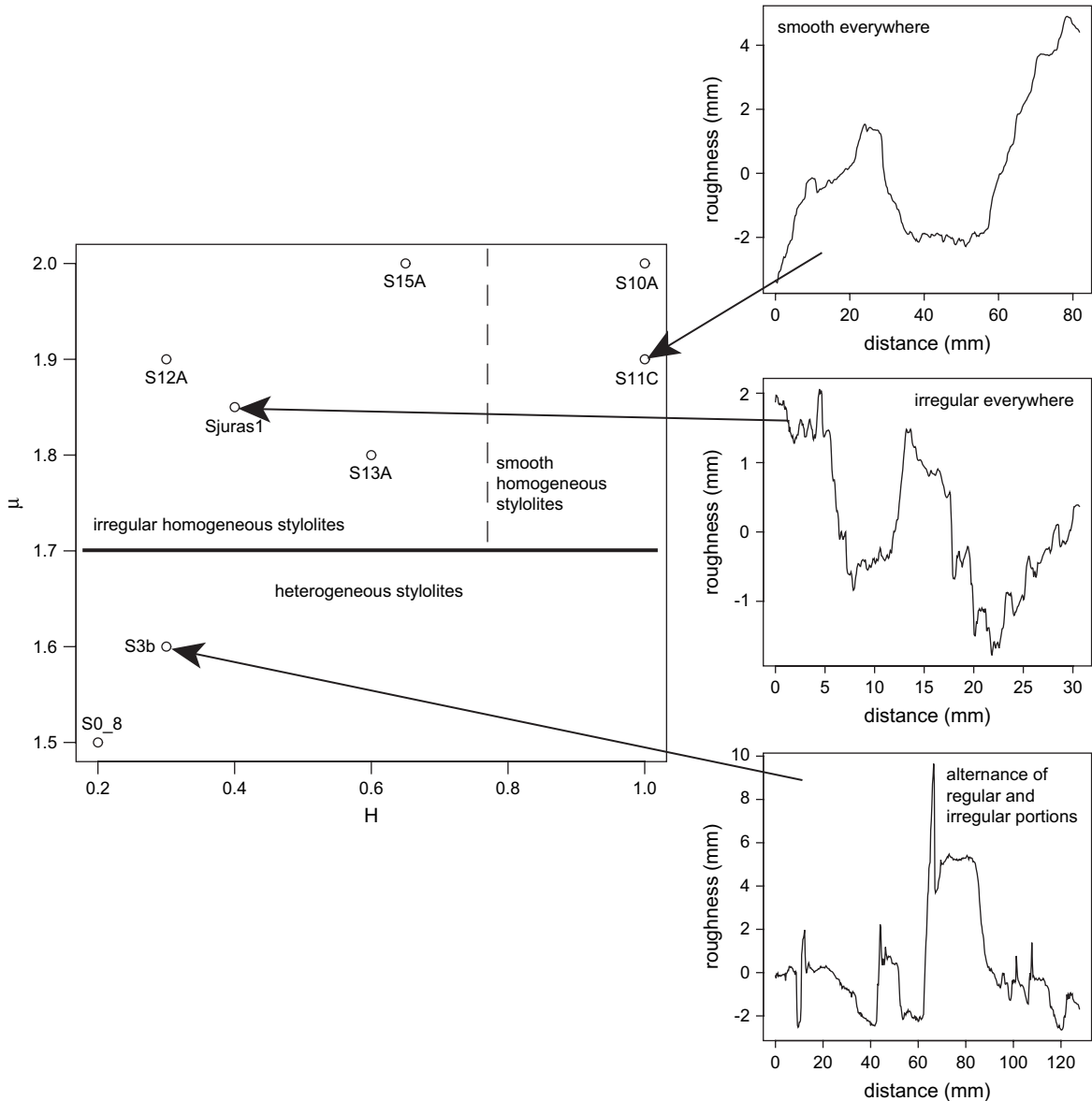


Fig. 9. Various morphologies of stylolites based on their statistical properties at large length scale. Two main families can be identified, based on their statistical properties: those which are either regular or irregular everywhere, and those with alternating regular and irregular portions.

stylolites are non-stationary. In this case, the initial heterogeneities in the rock that are reached by the stylolite during its propagation are recorded in the stylolitic signal. More exactly, above the millimeter scale, where elastic interactions dominate, heterogeneity may be seen in the signal. Below the millimeter scale, where surface tension dominates, this heterogeneity has disappeared.

Agglomerative nesting, clustering methods and principal component analysis (not shown here) have been performed and indeed show that statistical analysis supports the classification of stylolite morphologies in two different classes.

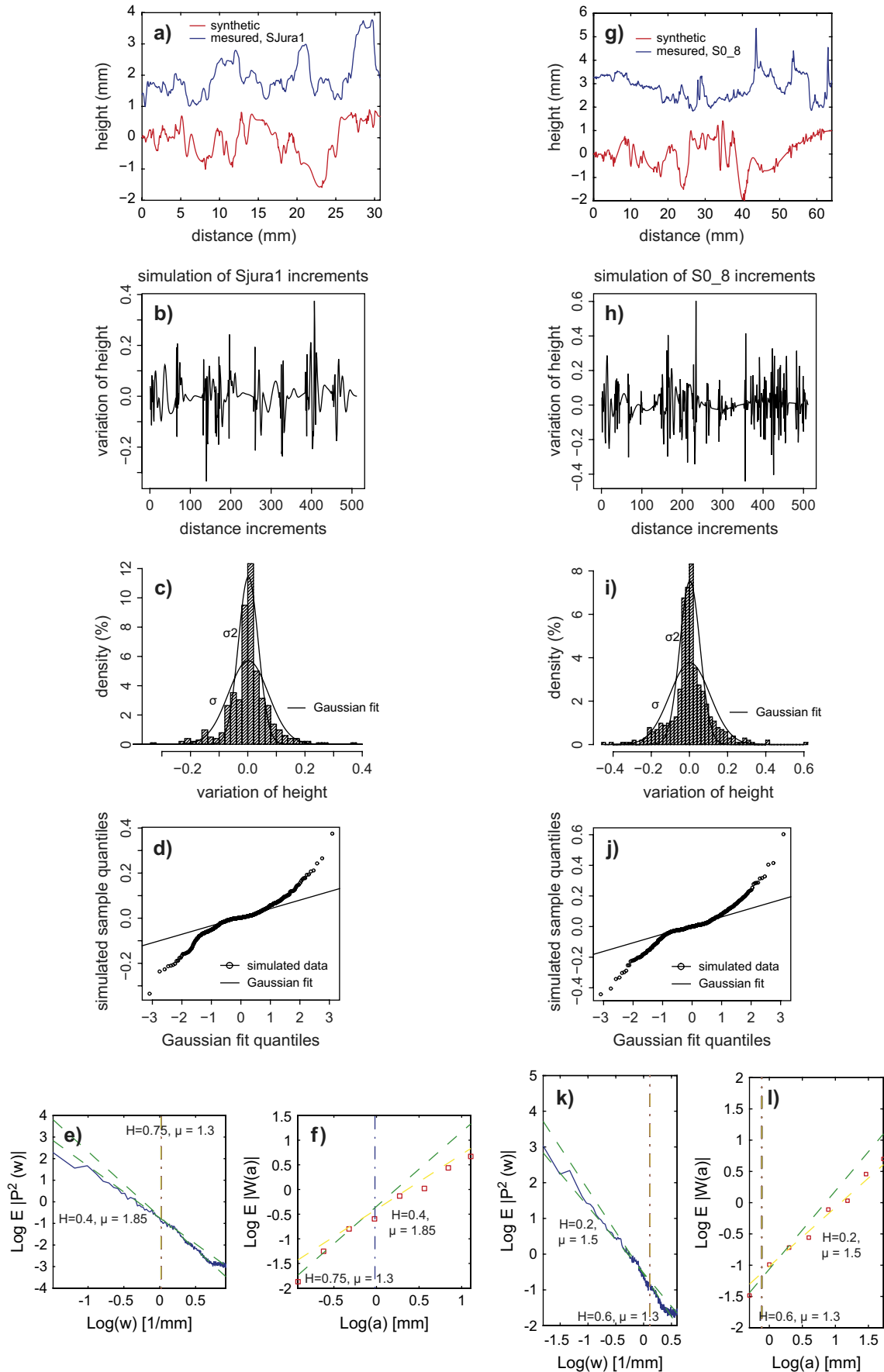
4.3. Simulations

Given a set of parameters (H , μ) for both regimes (large and small length scale behaviors from both parts of the crossover

length scale), the behavior of all measured stylolites can be reproduced with two SBPWS. This technique can be used to simulate a wide range of stylolite morphologies (Figs. 7 and 10):

- those which are close to stationary profiles (μ close to 2);
- smooth profiles with H close to 1 to irregular profiles with a fractional exponent H ;
- more heterogeneous profiles with alternating smooth and irregular zones (where $\mu \neq 2$).

An interesting perspective would be to use the shape and regularity of stylolites in order to evaluate the heterogeneity of the rock before or during the stylolitic process, and therefore better characterize under which conditions (depth, cohesion of the sediment) stylolites form. Another perspective would be to choose a different noise (a fractional stable noise



for instance) in the Langevin growth equations proposed in Renard et al. (2004) and Schmittbuhl et al. (2004). This remains a real prospect for continuous stylolites' models and, more generally, a theoretical extension of rough surface growth models.

5. Conclusions

When the increments of a mathematical function are not stationary (in other words their statistics vary along the coordinate), or the variance of their distribution is infinite, standard tools (Fourier spectrum or average wavelet coefficient analysis) fail to capture a roughness property from a scaling property.

Therefore, an extension of such tools to non-stationary signals is proposed here by using a two-parameter approach. One of the parameters, the local roughness exponent H , describes the noisiness or waviness of the signal. The second parameter, μ , describes how the statistical properties vary along the signal.

Applied to stylolites, two kinds of geometry can be distinguished.

- i) Stationary stylolites, where the statistics do not vary along the stylolite. For this kind of stylolite, two sub-families can be defined: stylolites that are almost flat everywhere and those that are very wavy everywhere.
- ii) Non-stationary stylolites where wavy portions alternate with flatter ones. In this case, we propose that heterogeneities initially present in the rock strongly control the stylolite morphology. To our knowledge, this second kind of stylolite, which has fossilized the heterogeneities of the rock in its morphology, has not been previously quantified. Detailed microstructural and chemical mapping studies focusing on the characterization of heterogeneities around stylolites would surely bring new information.

This difference between the two families of stylolites is detected only for wavelengths greater than a crossover scale close to the millimeter. Below this scale, the statistics of all the stylolites are very homogeneous, indicating that a physical process, probably driven by the minimization of the local curvature, smoothes the stylolites at small scales.

Acknowledgments

This project was supported by the CNRS (ATI and DyETI programs).

Appendix A. Algorithm to build synthetic signals

```

%////////// Run the styloprocess function ////////////
%Matlab® program to create the stylolites of Figure 7
%Parameters of the simulation
%K: depth of the tree (2^K+1 is the number of points on
the profile)
%mu: heterogeneity parameter (between 1 and 2)
%H: local roughness exponent (between 0 and 1)

function (stylolite) = styloprocess (K,mu,H)

x=linspace(0,2,2^(K-1));
Y=1-abs(x-1);
psi=(-Y,Y,0);
trees=createtree(K,(2-mu));
profile=reconstruct(K,trees,H,psi);
plot(profile);

%////////// Galton-Watson Tree ////////////
function (trees)=createtree(K,p)

randn('state',sum(100*clock));
trees(1)=randn(1);
for m=0:K-1
    for l=0:2^m-1
        zfather=2^m+1;
        zson1=2*zfather;
        zson2=2*zfather+1;
        if (trees(zfather)==0)
            trees(zson1)=0;
            trees(zson2)=0;
        else
            if (rand(1)<p)
                if (rand(1)<1/2)
                    trees(zson1)=randn(1);
                    trees(zson2)=0;
                else
                    trees(zson2)=randn(1);
                    trees(zson1)=0;
                end
            else
                trees(zson1)=randn(1);
                trees(zson2)=randn(1);
            end
        end
    end
end
end

%////////// Reconstruction ////////////
function (sig)=reconstruct(K,trees,H,psi)

sig=zeros(1,2^K+1);
for m=0:K
    psim=[];
    for j=1:2^(K-m)+1
        psim(j)=2^(m/2)*psi(2^m*(j-1)+1);
    end
    sigtemp=[];
    for l=0:2^m-1;
        zfather=2^m+1;
        psitemp=2^(-m*(H+1/2))*trees(zfather)*psim;
        sigtemp=[sigtemp,psitemp(2:2^(K-m)+1)];
    end
    sig=sig+sigtemp;
end

```

Fig. 10. Using both values H and μ estimated at large length scale and at small length scale, one can reproduce different morphologies of stylolites using a combination of two SBPWS behaviors. a) Profile of the stylolite Sjur1 (see Table 1) and synthetic profile with the same parameters at small and large length scales as those estimated on Sjur1. b) Derivative of the synthetic signal of a) showing the increments. c) Histogram of the simulated increments. d) Quantile–quantile plot, as in Fig. 5 showing the departure from a Gaussian distribution. FPS (e) and AWC (f) spectra analysis for the synthetic signal having the same statistical properties as Sjur1. The green dashed straight lines at small and large length scales indicate the estimated slopes, showing the two characteristic slopes and the crossover length scale. g,l) Stylolite S0_8 and synthetic profiles with the same parameters as estimated on S0_8 and similar analysis than in a,d). FPS (g) and AWC (h) spectra of the synthetic stylolite showing the two characteristic slopes and the crossover length scale.

Appendix B. Calculation of H and μ on 1D signals

A 1D profile $h(x)$ is observed on a regular grid (at space $x_i = i/2^n$ for $i = 0 \dots 2^n - 3$). Note the second order variation, an approximation of the second order derivative, at point x_i , by

$$\Delta_a h\left(\frac{i}{2^n}\right) = \sum_{l=0}^2 a_l h\left(\frac{i+l}{2^n}\right) \quad (\text{B1})$$

where $a = (a_0, a_1, a_2) = (-1, 2, -1)$.

Summing the $2^n - 3$ variations $\Delta_a h(i/2^n)$ for $i = 0 \dots 2^n - 3$, the statistic $V_{n,s}$ is obtained

$$V_{n,s} = \sum_{i=0}^{2^n-3} \left(\Delta_a h\left(\frac{i}{2^n}\right) \right)^s \quad (\text{B2})$$

where $s = 2$ (also called quadratic variations) or $s = 4$ (quadratic variations). This statistics behaves according to a power law depending on the parameters H and μ , with $V_{n,s} \approx 2^{n(sH - \log_2 \mu)}$.

If we note,

$$W_{n,s} = \log_2 \left(\frac{V_{n-1,s}}{V_{n,s}} \right) \quad (\text{B3})$$

then $W_{n,s} \xrightarrow{n \rightarrow \infty} sH - \log_2 \mu$ and by linear combination, either μ or H is obtained. The estimators are, respectively,

$$\mu_n = 2^{W_{n,4} - 2W_{n,2}} \quad \text{and} \quad H_n = \frac{1}{2}(W_{n,4} - W_{n,2}). \quad (\text{B4})$$

References

- Barabási, A.L., Stanley, E.H., 1995. *Fractal Concepts in Surface Growth*. Cambridge University Press, New York.
- Bathurst, R., 1971. *Carbonate Sediments and Their Diagenesis*. Elsevier Science, New York.
- Bayly, B., 1986. Mechanisms for development of stylolites. *Journal of Geology* 94, 431–435.
- Brouste, A., 2006. Etude d'un processus bifractal et application statistique en géologie. Ph.D. thesis, Université Joseph Fourier, Grenoble, France, 180 p.
- Cerasi, P., Mills, P., Fautrat, S., 1995. Erosion instability in a non consolidated porous medium. *Europhysics Letters* 29, 215–220.
- Daubechies, I., 1992. *Ten Lectures on Wavelets*. Society for Industrial and Applied Mathematics, Philadelphia.
- Dunne, T., 1980. Formation and controls of channel networks. *Progress in Physical Geography* 4, 211–239.
- Dunnington, H., 1954. Stylolites development post-date rock induration. *Journal of Sedimentary Petrology* 24, 27–49.
- Feder, J., 1988. *Fractals*. Plenum Press.
- Fletcher, R.A., Pollard, D.D., 1981. Anticrack model for pressure solution surfaces. *Geology* 9, 419–424.
- Gratier, J., Muquet, L., Hassani, R., Renard, F., 2005. Experimental microstylolites in quartz and modeled application to natural stylolitic structures. *Journal of Structural Geology* 27, 89–100.
- Harris, T.E., 1963. *The Theory of Branching Processes*. Springer-Verlag, Berlin.
- Istas, J., Lang, G., 1997. Quadratic variations and estimation of the local Hölder index of a Gaussian process. *Annales de l'Institut Henri Poincaré* 33 (4), 407–436.
- Jaffard, S., 2000. On lacunary wavelet series. *Annales de l'Institut Henri Poincaré* 10, 313–329.
- Kahane, J.P., Lemarié-Rieusset, P.G., 1998. *Séries de Fourier et ondelettes*. Editions Cassini, Paris.
- Karcz, Z., Scholz, C.H., 2003. The fractal geometry of some stylolites from the Calcare Massiccio Formation, Italy. *Journal of Structural Geology* 25, 1301–1316.
- Katsman, R., Aharonov, E., Scher, H., 2006. A numerical study on localized volume reduction in elastic media: some insights on the mechanics of anticracks. *Journal of Geophysical Research* 111, B03204, doi:10.1029/2004JB003607.
- Koehn, D., Arnold, J., Malthe-Sørensen, A., Jamtveit, B., 2003. Instabilities in stress corrosion and the transition to brittle failure. *American Journal of Science* 303, 956–971.
- Meakin, P., 1998. *Fractals: scaling and growth far from equilibrium*. Cambridge University Press, New York.
- Meyer, Y., Roques, S., 1993. Progress in wavelets analysis and applications. In: *Proceedings of the International Conference "Wavelets and Applications"*. Editions Frontières.
- Park, W., Schot, E., 1968. Stylolites: their nature and origin. *Journal of Sedimentary Petrology* 38, 175–191.
- Samorodnitsky, G., Taqqu, M.S., 1994. *Stable Non-Gaussian Random Processes: Stochastic Models with Infinite Variance*. Chapman and Hall, New York.
- Schmittbuhl, J., Gentier, S., Roux, S., 1993. Field measurements of the roughness of fault surfaces. *Geophysical Research Letters* 20, 639–641.
- Schmittbuhl, J., Renard, F., Gratier, J.-P., Toussaint, R., 2004. The roughness of stylolites: implications of 3D high resolution topography measurements. *Physical Review Letters* 93, 238501.
- Simonsen, I., Hansen, A., Nes, O.M., 1998. Using wavelet transforms for Hurst exponent determination. *Physical Review E* 58, 2779–2787.
- Renard, F., Schmittbuhl, J., Gratier, J.-P., Meakin, P., Merino, E., 2004. Three-dimensional roughness of stylolites in limestones. *Journal of Geophysical Research* 109, B03209, doi:10.1029/2003JB002555.
- Rubio, M.A., Edwards, C.A., Dougherty, A., Gollub, J.P., 1989. Self-affine fractal interface from immiscible displacement in porous media. *Physical Review Letters* 63, 1685–1688.